



ELSEVIER

Biophysical Chemistry 72 (1998) 21–35

Biophysical  
Chemistry

## Propagating waves control *Dictyostelium discoideum* morphogenesis

Dirk Dormann, Bakhtier Vasiev, Cornelis J. Weijer\*

*Department of Anatomy and Physiology, University of Dundee, Dundee, DD1 4HN, UK*

Revision received 16 January 1998; accepted 13 February 1998

### Abstract

The morphogenesis of *Dictyostelium* results from the coordinated movement of starving cells to form a multicellular aggregate (mound) which transforms into a motile slug and finally a fruiting body. Cells differentiate in the mound and sort out to form an organised pattern in the slug and fruiting body. During aggregation, cell movement is controlled by propagating waves of the chemo-attractant cAMP. We show that mounds are also organised by propagating waves. Their geometry changes from target or single armed spirals during aggregation to multi-armed spiral waves in the mound. Some mounds develop transiently into rings in which multiple propagating wave fronts can still be seen. We model cell sorting in the mound stage assuming cell type specific differences in cell movement speed and excitability. This sorting feeds back on the wave geometry to generate twisted scroll waves in the slug. Slime mould morphogenesis can be understood in terms of wave propagation directing chemotactic cell movement. © 1998 Elsevier Science B.V. All rights reserved

**Keywords:** Cell movement; Wave propagation; Chemotaxis; Morphogenesis; Spiral waves

### 1. Introduction

A major goal in the study of development of eukaryotic organisms is to understand the mechanisms of morphogenesis, i.e. how does a complex organism develop from a single cell, the fertilised egg and what determines its final shape. Mechanisms responsible for the development of multicellular organisms involve spatiotemporal control of cell proliferation, cell death and cell differentiation as well as differential cell movement. These processes have to be precisely controlled in space and time and furthermore they have to be stable against external perturbations.

This control involves extensive cell-cell signalling via extracellular factors. They interact in characteristic positive and negative feedback circuits to result in the spatiotemporal regulation of different cellular processes.

We have focused on the study of the morphogenesis of a very simple organism, the cellular slime mould *Dictyostelium discoideum*. Slime moulds are positioned between uni- and multi-cellular life in the evolutionary tree. *Dictyostelium* undergoes a multicellular development (Fig. 1) which shows many of the characteristic features of the development of higher organisms, such as cell differentiation and differential chemotactic cell movement to put the cells in the right place.

Slime moulds live as single amoebae in the soil where they feed on bacteria and divide by binary fis-

\* Corresponding author. Tel.: +44 1382 345191; fax: +44 1382 345514; e-mail: cj.weijer@dundee.ac.uk

sion. Starvation induces the activation of a developmental program in which the cells aggregate chemotactically to form a multicellular mass of  $10^4$ – $10^5$  cells. Since multicellular development occurs in the absence of food there is little cell division, thus simplifying the analysis of morphogenesis [1,2]. In the aggregate (mound) the cells start to differentiate into a number of different cell types, i.e. several prestalk types which will form the stalk and the basal disk, upper and lower cup of the fruiting body as well as prespore cells which will differentiate into spores. Differentiation occurs at random positions in the late aggregate [3] and the prestalk cells sort out chemotactically to form the tip of the 'tipped' mound [4]. The mound erects and extends up in the air to form the standing slug which falls over and migrates away. The slug has a distinct polarity with a tip at the anterior end which guides its movement. The slug is photo- and thermotactic which allows it to move up towards the soil surface. There it transforms into a small fruiting body (up to 4 mm high) consisting of a stalk supporting a spore mass. The spores disperse and under suitable conditions they germinate to release amoebae and the whole cycle can start all over again. In this article we will give an overview of the mechanisms that control aggregation, mound and slug formation and show that these processes can be viewed as pattern formation in a biological excitable system.

## 2. Aggregation

The principles that govern aggregation are now relatively well understood at the cellular level. Aggregation of individual *Dictyostelium* amoebae into multicellular aggregates occurs by chemotaxis to 3',5'-cyclic adenosine monophosphate (cAMP). The cells in the aggregation centre periodically synthesise and release cAMP in the extracellular medium. Here it diffuses to neighbouring cells which detect this signal via highly specific and very sensitive cAMP receptors. These receptors are transmembrane proteins with an extracellular cAMP binding domain and an intracellular effector domain. Binding of cAMP to the receptor triggers two competing processes, excitation and adaptation (reviewed in Ref. [5]). The excitation pathway leads to the activation of the enzyme adenylyl cyclase, which produces cAMP. It involves at

least one heterotrimeric G protein, a cytosolic protein called cytosolic regulator of adenylyl cyclase (CRAC) as well as a MAP kinase [5]. This intracellular cAMP is secreted to the outside where it can bind to the receptors of the same cell generating an autocatalytic feedback, but it also diffuses away to activate neighbouring cells. The adaptation pathway involves the desensitisation of the receptor, resulting in a termination of the autocatalytic relay response. It has been shown that desensitisation is accompanied by receptor and G protein phosphorylation on several serine residues in its cytoplasmic tail. However it has also been shown that this phosphorylation is not essential for desensitisation and the precise molecular mechanism is still unknown [5,6]. Moreover, the cells secrete an enzyme cAMP phosphodiesterase which degrades cAMP [7]. The fall in the extracellular concentration of cAMP leads to the dephosphorylation and resensitisation of the receptor. The adaptation process is responsible for the outward propagation of cAMP waves, since cells which have just relayed the signal are refractory to further stimulation by cAMP. cAMP also causes a chemotactic reaction in the direction of higher cAMP concentrations. The cells move up the gradient as long as the cAMP level is rising but stop to move as soon as the concentration starts to decrease. This mechanism is responsible for the periodic movement of the cells towards the aggregation centre guided by the propagated cAMP waves. Superimposed on this system there is a complex feedback of the cAMP oscillations on the expression of various components of the signalling system. cAMP pulses induce the synthesis of cAMP receptors, adenylyl cyclase and phosphodiesterase resulting in an increase in excitability during aggregation [8,9].

During early aggregation the cAMP waves can be seen as optical density waves using low-power dark-field optics [10–12]. These optical density waves are correlated to shape changes which cells undergo upon stimulation with cAMP. Chemotactically moving cells are elongated and appear brighter than non-moving cells resulting in the appearance of dark and light bands in fields of aggregating cells (Figs. 1 and 2).

By correlating the cAMP signal via isotope dilution-fluorography with the dark-field waves, it was clearly demonstrated that the optical density waves observed during aggregation represent the propagat-

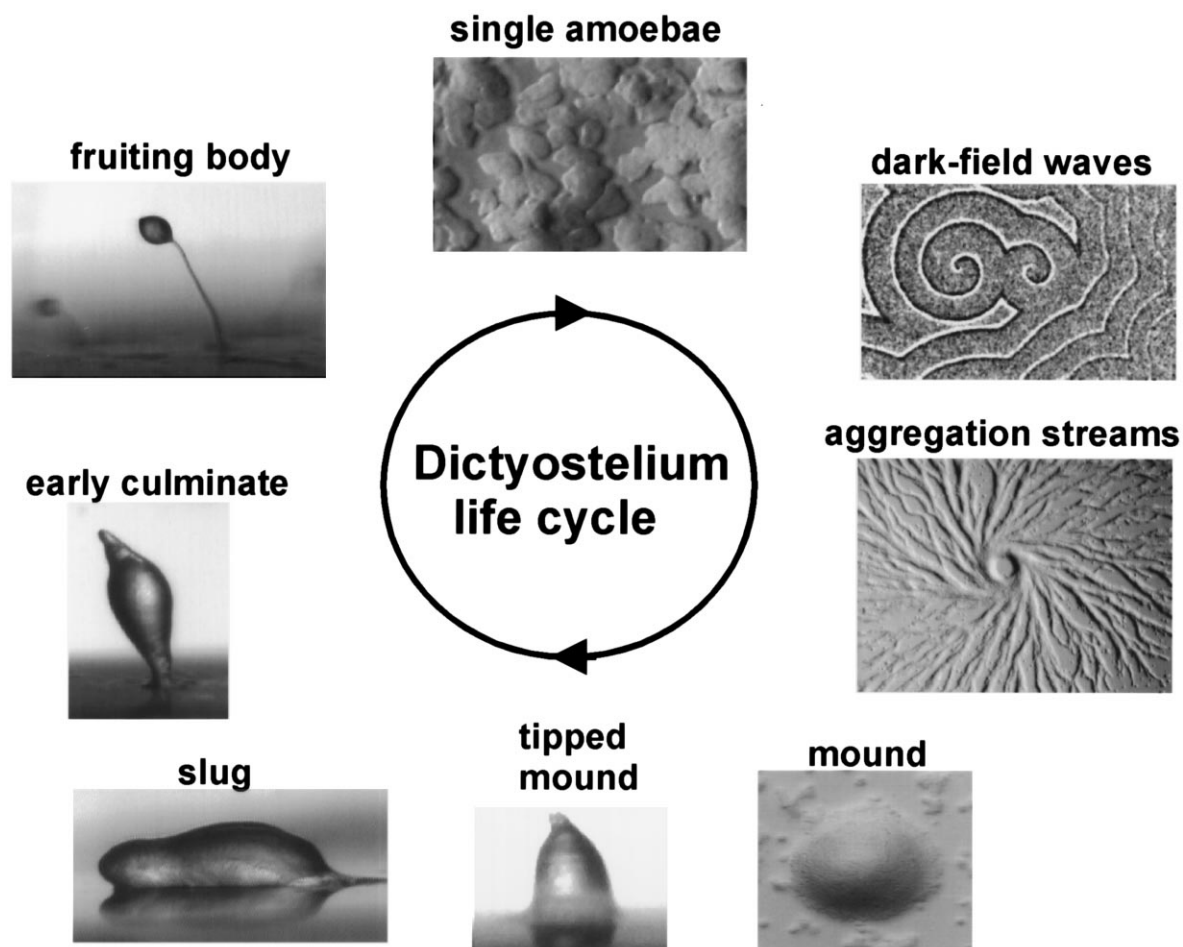


Fig. 1. *Dictyostelium* life cycle. Shown are single amoebae, dark-field waves, aggregation streams, mounds, a slug, an early culminate and a fruiting body. Development takes 24 h at room temperature.

ing cAMP signal [13]. Most often waves appear as expanding spirals, in some strains also as concentric ring waves. Waves from neighbouring centres collide and annihilate each other leading to the formation of aggregation territories. Quantitative measurements showed that the frequency of the waves increases during aggregation while the wave propagation speed slows down. This is partly due to the cAMP dependent expression of components of the oscillatory system as well as to the dispersive properties of this excitable medium [8,14,15].

There have been several attempts to model the early aggregation process. Two main questions need to be addressed: how do the cells produce cAMP waves and

how do they move in response to these waves? Essentially two types of models were developed to describe mathematically the cAMP relay kinetics of *Dictyostelium* amoebae. The first model has been suggested by Martiel and Goldbeter [16–18]. It is based on the assumption that activation/inactivation of the cAMP receptors plays a key role in the response. A second model has been introduced by Tang and Othmer [19]. In this model the receptor dependent activation of activating and inhibitory G proteins controls the periodic cAMP production. Both models are able to describe oscillations in the cAMP level in cell suspensions as well as cAMP wave propagation in a dispersed cell population [14,20]. These models

basically describe excitable and/or oscillatory media and are very similar to the prototype FitzHugh–Nagumo system:

$$\begin{aligned}\partial g/\partial t &= D\Delta g - \rho(k_g g(g - 0.05)(g - 1) + k_r r) \\ \partial r/\partial t &= (g - r)/\tau\end{aligned}\quad (1)$$

The first equation describes the excitation of the medium, defined by the variable ( $g$ ), over time. This variable is linked to the extra cellular cAMP concentration. The second equation defines the recovery process of the medium ( $r$ ) and could be thought to describe the desensitisation of the cAMP receptors.  $D$  is the diffusion coefficient for cAMP;  $\tau$  is a time scaling factor for the variables  $r$  and  $g$ ;  $k_g$  and  $k_r$ , define the rate of production and hydrolysis of cAMP by one cell. The effect of cell density on the excitability of the medium is accounted for by the factor  $\rho$ , which scales the excitability of the medium (rate of production of cAMP).

cAMP waves not only propagate through the cell

population but also coordinate cell movement. cAMP orients the direction of otherwise randomly moving cells. There is strong evidence that the cells detect the gradient of cAMP over their length [21–23]. However, there is also evidence that cells use the temporal derivative of cAMP and only move up the gradient as long as the cAMP level is rising [24,25]. This allows cells to move chemotactically on the wave front rather than on the wave back. A number of mathematical models have been proposed for chemotactic cell movement. The best known one is the Keller–Segel model [26] describing a cell flux,  $J$  as a function of cell density,  $\rho$ , and concentration of cAMP,  $g$ .

$$J = -D(g)\nabla\rho + \chi(g)\rho\nabla g\quad (2)$$

The first term on the right hand side describes random cell movement (the velocity can depend on the level of cAMP) and the second term the directed motion of the cells along the cAMP gradient. There exist also a number of models where chemotactic cell motion is described in an axiomatic way as rules for motion of

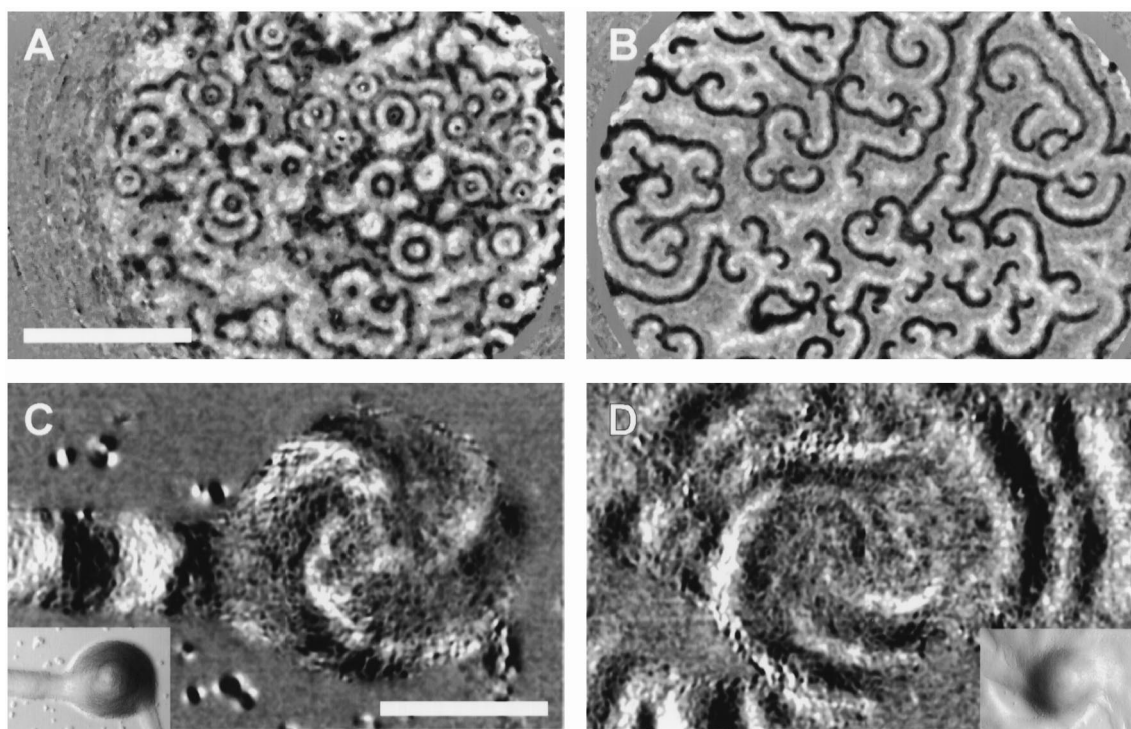


Fig. 2. Different modes of signal propagation in two different strains  $Ax_3$  (B,D) and DH1 (A,C). (A,B) Aggregation stage cells showing typical spiral waves in  $Ax_3$  (B) and target patterns in DH1 (A). (C,D) Three-armed spirals observed in mounds of both  $Ax_3$  (D) and DH1 (C). Panels (A,B) are on the same scale given by the white bar in (A) (10 mm); (C,D) are on the same scale given by the bar in (C) (250  $\mu\text{m}$ ).

units (cells) in a concentration field of cAMP [27–30].

Much effort has been directed towards understanding the physical principles leading to the formation of streaming patterns by amoebae responding chemotactically to propagating cAMP waves. It has been shown analytically and numerically that streams form due to a streaming instability caused by a coupling between the velocity of signal propagation and density of cells [30–34]. This is presumably related to the angular instability as discussed by Shaffer and Nanjundiah [35,36]. Local accumulation of cells will, due to the dependence of the rate of cAMP accumulation on cell density, result in a speeding up of the wave propagation. This local deformation of the wave front will lead to the attraction of even more cells to this region and finally to the formation of bifurcating aggregation streams [30,32,34], in which the cells move towards the aggregation centre. There they pile on top of each other to form a 3D hemispherical structure, the mound. In the streams the cells are elongated and connected by rather characteristic end to end contacts. The movement of individual cells however is still periodic, but somewhat faster than that of isolated cells, possibly suggesting a cooperative effect on their movement [37].

### 3. Wave propagation and cell movement in mounds

Special image processing techniques allowed us to visualise propagating optical density waves in the later stages of *Dictyostelium* development. We can visualise optical density waves in aggregation streams and mounds [38,39]. Continuous measurements of the optical density waves from late aggregation until tip formation over a period of 3 h demonstrated that there was a clear evolution in the dynamics of the waves [39]. Initially the waves propagate fast at low frequency but in the course of aggregation the wave frequency increased, while the wave propagation speed decreased. Although we can observe a continuous succession of optical waves from aggregation to the mound stage it is not proven that the waves in the mound are caused by chemotaxis to propagating cAMP signals. Periodic microinjection of pulses of cAMP into the extracellular space in mounds initiated

optical density waves which propagated from the electrode tip outwards and which interacted with endogenous waves (Rietdorf, Siegert and Weijer, unpublished data). These observations clearly show that optical density waves in mounds can be induced by cAMP oscillations and furthermore that induced waves annihilate endogenous waves upon collision, showing a common propagation mechanism.

In the mound stage the geometry of the waves can be very variable. The pattern of wave propagation seems to be a characteristic of the strain used. We have found a variety of different wave propagation patterns in mounds. Some strains predominantly show concentric ring waves [38]. These waves can originate from one centre in the mound. In some cases we found that the mound behaves as a very excitable medium in which target waves arise simultaneously from a number of different centres, the location of which may change in time and space during development. The waves generated by these centres compete and interact during the development of the mound and finally one centre seems to become dominant. We also observed simple spiral waves in mounds. In some strains the geometry of the spirals can be more complicated and result in the formation of multi-armed spirals [38,39].

We have observed single and multi-armed spirals in the strains Ax<sub>2</sub> and Ax<sub>3</sub>. The strains that produce spirals in mounds are also strains that produce spirals during aggregation. The diverse geometry of the signals leads to a variety of complex cell motion patterns. Since cell movement is always opposite to the direction of signal propagation [10,39] cell movement in mounds organised by concentric waves is directed towards the organising centre and slow, while in the case of spiral waves, cell movement is rotational and fast.

More recently we have started to investigate another strain, DH1. This is an uracil auxotroph derived from Ax<sub>3</sub> in which the pyr5,6 gene coding for UMP synthase has been disrupted [40,41]. This strain has been used extensively as a parent strain to generate mutants in essential signal transduction components such as cAMP receptors and cAMP phosphodiesterase. It is supposed to be wildtype when grown in the presence of uracil. We found that this strain showed a number of interesting features during aggregation and mound formation. During the early stages

of aggregation it always produced target pattern type waves. This is different from the strain  $Ax_3$  from which it was derived, which always produces spiral waves during early aggregation (Fig. 2A,B). In the

mound stage this strain just as  $Ax_3$  and another axenic mutant  $Ax_2$  produces multi-armed spiral waves (Fig. 2C,D). This shows that during the development of *Dictyostelium* cells the kinetics of the relay reaction

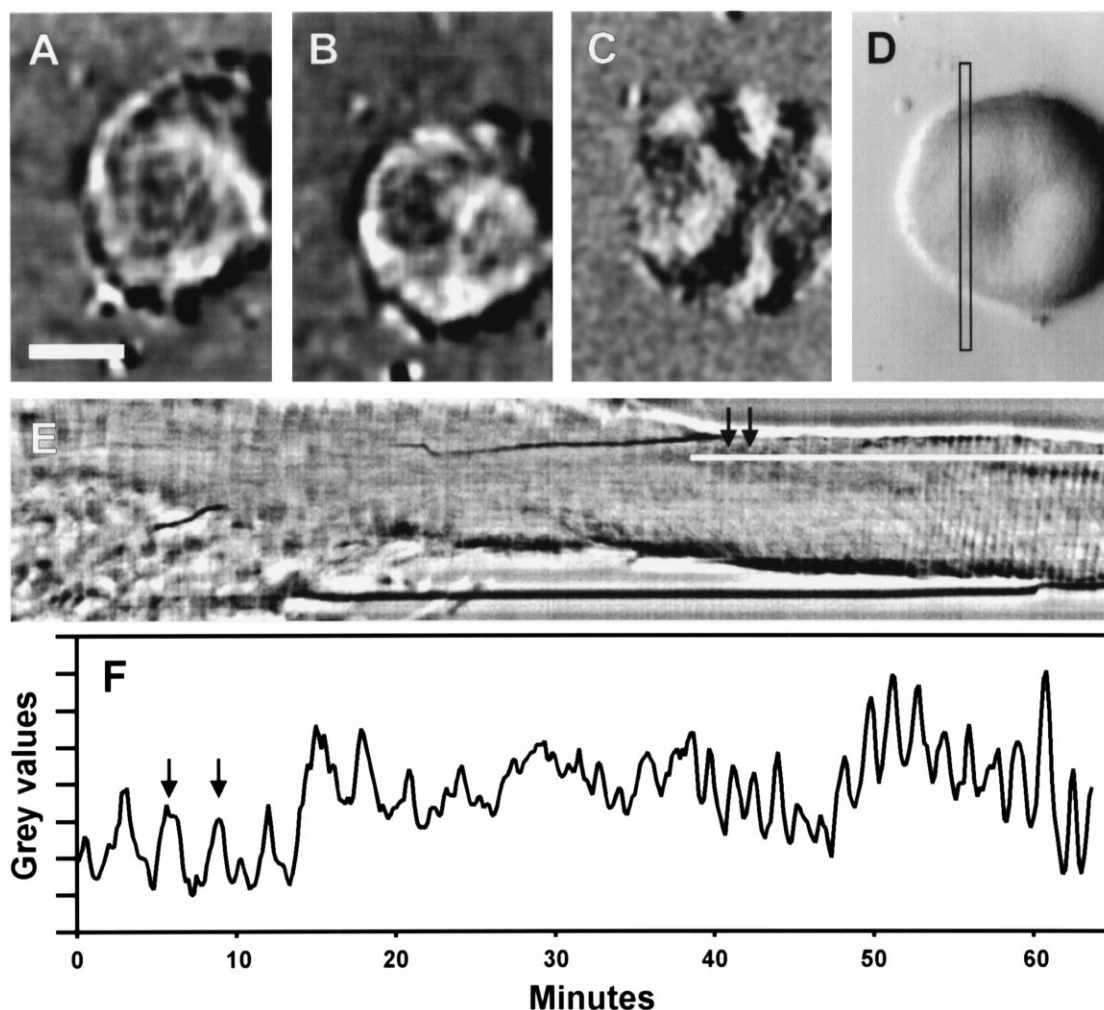


Fig. 3. The transition from concentric ring waves to multi-armed spirals in strain DH1. (A) Image of a mound in an early stage of the transition from a concentric ring wave to a single-armed spiral. The image is generated by subtracting successive images as detailed in Ref. [39] to visualise the waves. The white scale bar represents 100  $\mu\text{m}$ . (B) Image of the same mound some 60 min later showing a well developed single-armed spiral. (C) The same mound yet another 60 min later showing the existence of a five-armed spiral. (D) A transmitted light image of the mound shown in (C) before image processing to enhance the visibility of the waves. (E) Time-space plot generated from a time sequence of images of the same mound during the development of target patterns to single armed spirals into a multi-armed spiral (the images shown in (A,B) and (C) are taken at times corresponding to the beginning, the middle and the end of the time space plot shown in (E), respectively; the black window in (D) indicates the position where the time space plot was generated. (F) Trace of optical density against time recorded from the time space plot (E) along the horizontal white line in the upper right hand part of (E). It shows the change in frequency from around 3 min (the interval between the two black arrows in (E) and (F)) of the single armed spiral wave to a frequency of around 1.5 min at the five-armed spiral stage existing at the end of the sequence. It can be seen that there is a short chaotic transition period between the two.

changes to result in the transformation of target patterns into multi-armed spirals. We tried to analyse this process in more detail. The observation of DH1 showed that the target patterns break during the late aggregation stage and transform into single-armed spirals. These single-armed spirals are present for a period of 5–10 rotations after which they often transform into multi-armed spirals (Fig. 3A–D). We have not yet been able to resolve the precise geometry of the waves during the transition of single- to multi-armed spirals. However, it seems to occur very suddenly within a few rotations of the spiral wave (Fig. 3E,F). Measurement of the temporal dynamics of this evolution from time-space plots shows that during the time of the single-armed spirals the period of the oscillation is still low. In the example shown in Fig. 3E the period is around 200 s. During the transition it goes through a short period of chaotic behaviour after which five arms are formed. During the appearance of the extra arms the oscillation period decreases to 90–100 s. Wave propagation patterns of several mounds undergoing synchronous development on a plate all make the transition from single- to multi-armed spirals within the same time span of a few rotations. This indicates that the transition is triggered by a developmentally regulated event. It presumably reflects the appearance or disappearance of a new component of the signalling pathway which is strictly developmentally regulated.

Analysis of the pattern of cell movement has shown that the cells move in a direction opposite to the direction of wave propagation [39]. This can result in a considerable Doppler effect, i.e. the cells experience a higher oscillation frequency as the period we measure with respect to the laboratory coordinate system [42,43]. It could well be that the frequency increase seen by the cells is four- to five-fold during the transition of single to multi-armed spirals as expected theoretically during the transition from a one- to a four- or five-armed spiral.

Theoretical considerations have shown that these changes could explain the formation of multi-armed spirals from single-armed spirals during aggregation [44]. Model calculations showed that in low excitable media breakpoints in a single-armed spiral within one chemical wavelength from the core of the original spiral can lead to the formation of a double-armed spiral (Fig. 4). We also showed in these simulations

the number of arms in a multi-armed spiral depends on the ratio of the period of a single-armed spiral to refractoriness of the medium. This ratio has to be larger than the number of arms in the spiral [44].

One interesting characteristic of this developmental system is that the frequency increases continuously during development. During early development the period length of the target patterns (or spirals) might be 5–6 min. At the multi-armed spiral stage it goes down to less than 2 min. This implies that the signalling system is changing in time. Either the excitability increases or the refractoriness decreases or a combination of both. This would change the ratio of excitability to refractoriness and generate the conditions necessary for the formation of the multi-armed spirals by the mechanism shown in Fig. 4.

During further development the DH1 strain showed yet another form of very interesting behaviour. After the mounds had undergone the transition to the multi-armed spirals they started to show a depression in the centre and many of them started to open up and form rings (Fig. 5). In the rings several travelling waves were clearly seen. These waves developed from the waves seen in the multi-armed spirals. Again, we have not yet been able to completely resolve the transformation experimentally, however at least in some cases they seem to develop smoothly from multi-armed spirals. These ring structures can go through a number of cycles where they open up and close again and then continue to develop into slugs. In many cases rings can fuse with neighbouring rings if they are close together.

Observation of fluorescently-labelled cells showed that the waves in these rings direct counter rotational movement of the cells (not shown). In experiments where we labelled the cells with the prestalk cell specific vital dye neutral red we observed that the cells in the rings start to differentiate in prestalk (stained) and prespore (unstained) cells (not shown). Contrary to the situation seen in wild type strains where a significant number of the staining cells sort out to form the tip of the mound the staining cells in the rings remain distributed in a more or less random fashion. They do not sort out. After a variable time of rotation the rings can get thinner locally and break. The cells keep moving in the direction of the wave source and form a mound again. Alternatively, the ring will contract and form a mound. Then the cells will sort out to

form a tip and the structure continues to form a slug, which will migrate away and form a fruiting body. It can easily be understood why the cells do not sort out in the rings. The waves rotate around without the presence of a localised source. Therefore the cells cannot use this information to sort out. It re-mains however an open question why the rings are formed in the first place. This is the question of cause and effect. Do the cells not sort out because the signals are such that they will form a ring or do they form a ring as the result of an inability

of the cells to sort and as a result the signals can only form a ring.

#### 4. A model for mound formation

Observation of cells moving in mounds prompted theoretical investigations where the cell movement is considered as a flow of a viscous compressible liquid. This approach has been successfully used in a hydrodynamic model describing the whole process of

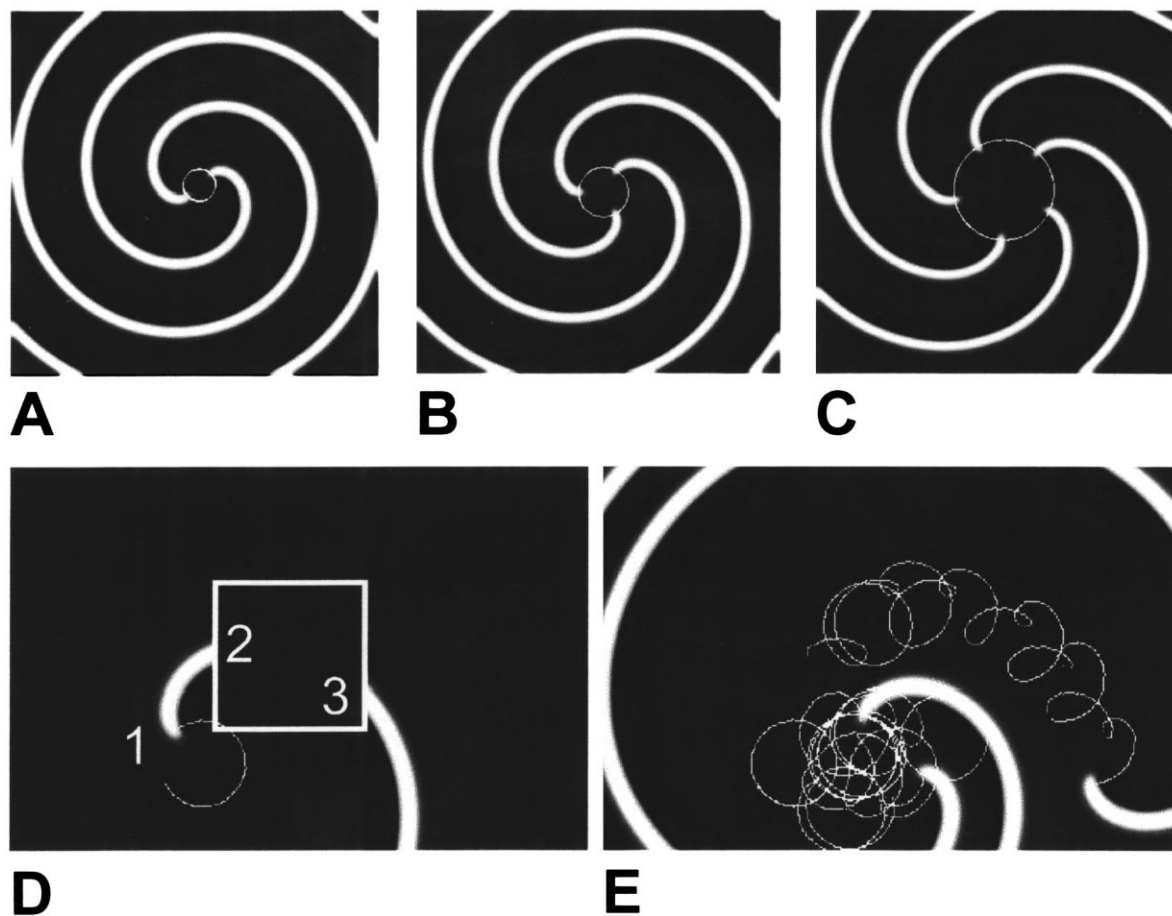


Fig. 4. Formation of multi-armed spirals in a 2D excitable medium described by the FitzHugh–Nagumo model Eq. (1). (A–C) Two-, three- and five-armed spirals are shown in media with different excitability. The possible number of arms increases with a decrease in the excitability of the medium. The dotted lines in the centre of the patterns indicate the path followed by the spiral tips. (D,E) Breaking of a single spiral can result in the formation of a two-armed spiral. It happens when the breakpoint is located not too far (within one chemical wavelength) from the spiral tip as in (D). The spiral tips 1 and 3 rotate in the same direction and attract each other to form a two-armed spiral. Spiral tip 2 rotates in opposite direction to 1 and 3 and is expelled from the medium as can be seen from the trajectories in (E). We assume that multi-armed spirals in the mound are formed via a similar mechanism. For initial conditions and parameter values see Ref. [73].



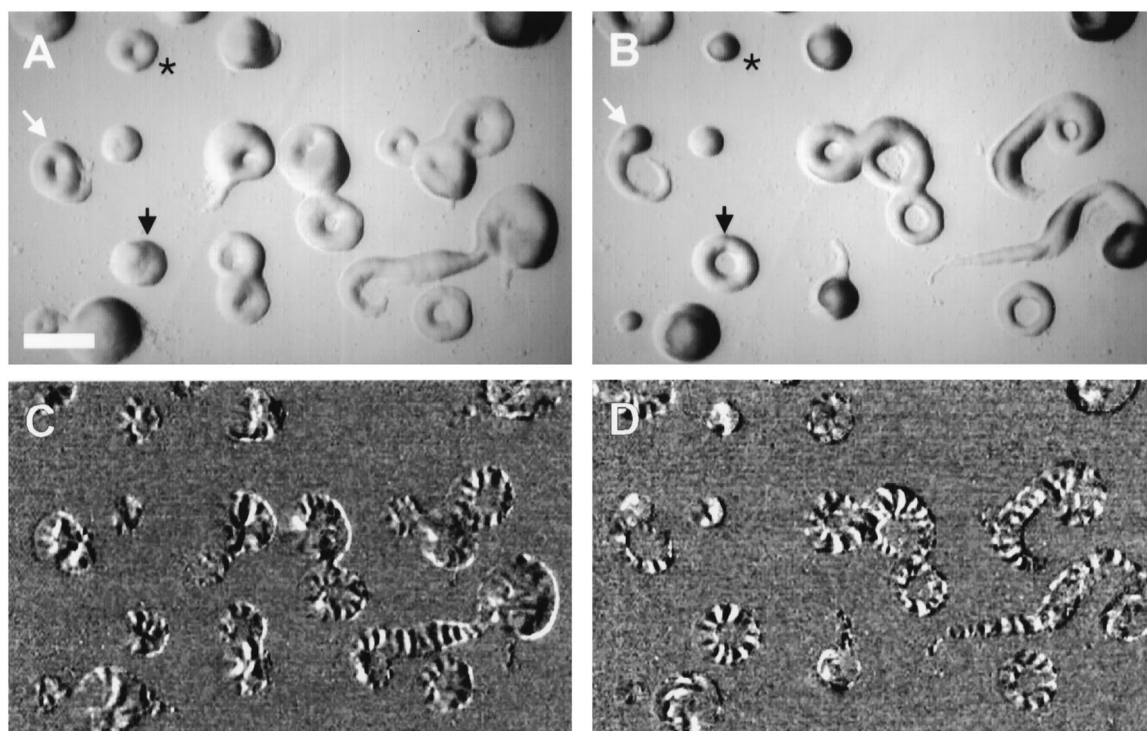


Fig. 5. Ring formation in the mutant DH1. (A,B) Two sequential images from a plate of DH1 cells. The images in (A) and (B) were taken 40 min apart. The bar in (A) represents 500  $\mu\text{m}$ . Seen are several mounds in the process of ring formation and ring closure as well as fusion and breaking. The ring marked by the white arrow in (A,B) is breaking. The mound marked by the black arrow in (A,B) is expanding into a ring, while the ring marked by the \* in (A,B) is contracting to a mound again. Some rings are seen in the process of fusion. (C,D) Subtraction images prepared from the images shown in (A) and (B) to visualise the wave patterns present in the various structures. It is clearly seen that many wave fronts are running through the mounds and rings. Many waves can be seen to bending concave back from the middle. This indicates the direction in which they are propagating.

aggregation until mound formation (Fig. 6). In this model cell velocity has been defined by the Navier–Stokes equation:

$$\rho[\partial V/\partial t + (V\nabla)V] = F_{\text{ch}} + F_{\text{fr}} + \eta\Delta V + \xi\nabla(\nabla V) + F_{\text{ad}} - \nabla p \quad (3)$$

The left hand side of the equation describes the acceleration of cells under the influence of various forces described on the right hand side of the equation.  $V$  is the velocity of the cells.  $F_{\text{ch}}$  is the chemotactic force which is active on the front of cAMP waves,  $F_{\text{fr}}$  is a friction force responsible for slowing down cell movement, The third and fourth terms on the right hand side describe cell-cell friction:  $\eta$  and  $\xi$  are viscosity coefficients.  $F_{\text{ad}}$  takes into account cell-cell and

cell-substrate adhesion forces,  $p$  is the pressure between the cells caused by the chemotactic accumulation of the cells (see Ref. [45] for details).

The evolution of the shape of the aggregate into a mound in this model has been obtained by solving an equation for the cell density field, i.e. by the equation for the conservation of mass:

$$\partial\rho/\partial t = D_{\rho}\Delta\rho - \nabla(\rho V) \quad (4)$$

The first term on the right hand side of the equation describes the random motion of the cells, while the second term describes coordinated chemotactic movement. Aggregation patterns found as solutions of Eq. (3), Eq. (4) in combination with the FitzHugh–Nagumo system Eq. (1) to describe the excitable cAMP kinetics are shown in Fig. 6.

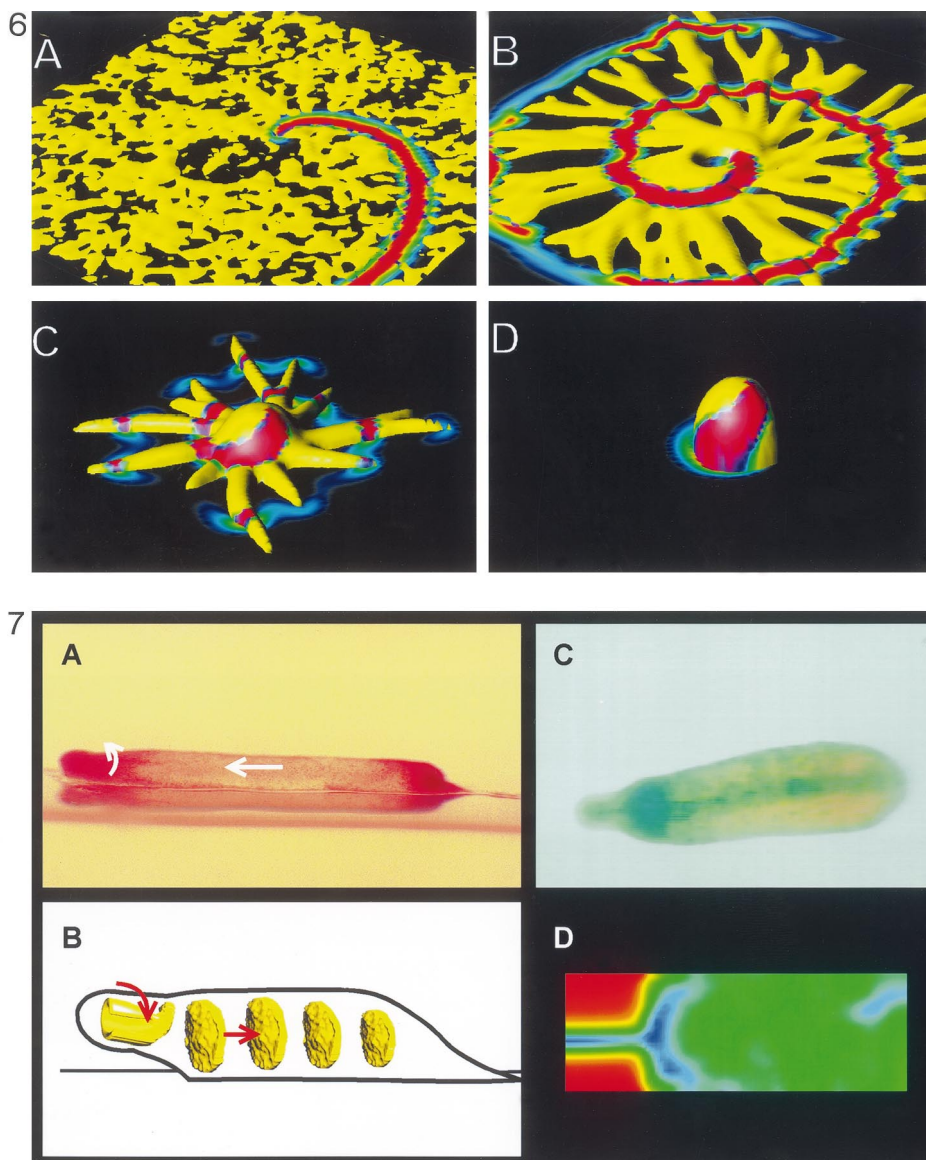


Fig. 6. Simulation of aggregation and mound formation using Eqs. (1) and (3). Cell density is shown as a yellow iso-surface ( $\rho = 0.5$ ) and the cAMP spiral is mapped on this surface (red). The initial density of cells was zero everywhere in 3D-space except for the bottom plane (A). The cell density in each grid of this plane was represented by a random number varying between 0 and 1 so that average density in this plane was equal to 0.5. In response to cAMP spiral wave cells move and form aggregation streams (B,C) and then mound (D) which represents a stable solution of the system. See Ref. [45] for details of the calculations.

Fig. 7. Wave propagation, cell movement and differentiation in slugs. (A) Photograph of a neutral red stained slug (side view). The dark stained region on the left hand side is the prestalk region. The arrows indicate the direction of cell movement. (B) Model for waves in the slug. The arrows indicate direction of cAMP wave propagation. (C) Photograph of a slug showing expression of the prestalk specific gene *ecmB* (blue region in slug), note the expression in the slug centre and at the prestalk-prestare boundary. (D) Average cAMP levels in the simulation after integration over ten periods of wave rotation. Note the close correspondence between average cAMP in the model (D) and cell type differentiation (A,C).

This model, although rather qualitative, shows some remarkable similarities with the formation and appearance of aggregates observed in real life (Fig. 1, Fig. 5). Furthermore it is able to describe some mutant phenotypes frequently observed [45].

## 5. Wave propagation in slugs

Up to the mound stage cAMP wave propagation can be seen as optical density wave using dark-field optics and digital image processing techniques [11,38]. It seems likely that periodic signals also control later development but it has not yet been firmly established that these signals are cAMP. In slugs of *Dictyostelium discoideum* we have not yet been able to observe propagating dark-field waves. During slug migration and culmination an extracellular slime sheath, which is secreted continuously, surrounds the slug. This gives the slug some mechanical stability but also impedes the observation of optical density waves. To find out whether periodic cAMP signals control slug migration and culmination, we investigated single cell behaviour and cell movement in multicellular structures, assuming that periodic signals should cause periodic cell movement. It was shown, that cells in the prespore zone of slugs go through periodic velocity and shape changes typical for chemotactically moving cells [46,47]. Further investigations showed, that there is a characteristic pattern of cell movement in *D. discoideum* slugs: cells in the prestalk zone show vigorous rotational movement around the central core of the tip, while cells in the prespore zone move straight forward in the direction of slug migration (Fig. 7A) [48]. From these observations the geometry of the propagating signal was deduced: a 3D scroll wave (spiral wave) causes rotational cell movement in the tip while planar wave fronts guide the straightforward movement observed in the prespore zone (Fig. 7B). We have observed optical density waves in slugs of the related species *Dictyostelium mucoroides* [49]. This species synthesises a stalk continuously during migration and forms long thin slugs which facilitate the visualisation of waves. Optical density waves are visible in the thin back region of the prespore zone of the slug (33). This species also uses cAMP as a chemo-attractant during the early stages and most likely also during later

stages of development [50]. Based on these data we proposed that the periodic signal in slugs was most likely cAMP. Recently experiments have been reported that show that an adenylate cyclase null mutants that overexpresses the catalytic subunit of the cAMP dependent protein kinase can aggregate at high cell densities and continue development to form mounds and slugs [51]. This seems to indicate that either slugs can form in the absence of cAMP waves or that there is another adenylate cyclase that takes over its role during development. Alternatively it might imply that adenylate cyclase is absolutely required for slug formation but controls slug formation normally. Since there is a lot of evidence that cAMP is involved in later morphogenesis both in the control of cell movement (cell sorting [52]) and in the control of differentiation [9] we still assume that cAMP normally controls cell movement not only in mounds but also in slugs.

Computer simulations showed that the conversion of a scroll into a series of planar waves occurs, if there is a substantial difference in excitability between the prestalk and prespore cell population [53]. This may be due to a difference in excitability between prestalk and prespore cells as possibly indicated by the cell type specific differences in the number and type of cAMP receptors adenylate cyclase and phosphodiesterase [54–57]. In the extreme case it might be caused by relaying of signal by prestalk and anterior-like cells only. This would imply that 100% of the cells in the prestalk zone relay the signal while in the prespore zone only the 15% randomly scattered anterior-like cells would relay the signal. This would give a good explanation for the existence of anterior-like cells [58].

During the slug stage there is a further specification of cell types. pstA cells are formed in the anterior outer part of the prestalk zone. pstO cells are found at the boundary between prestalk and prespore cells, while pstB cells, which will form the stalk, are found in the central core of the prestalk zone. The prespore cells are located in the back two-thirds of the slug [59]. Prespore genes need cAMP for their induction and stabilisation. Expression of the prestalk specific *ecmB* gene by the pstB cells is inhibited by high concentrations of extra cellular cAMP while *ecmA* expression by pstA cells requires high concentrations of cAMP [60–62]. Computer simulations using the

Martiel–Goldbeter model for cAMP oscillations showed, that the core of the scroll wave in the prestalk zone is a region of low average extracellular cAMP, exactly the condition which facilitates the expression of the stalk specific *ecmB* gene in the central core of the prestalk zone (Fig. 7C) [58]. Despite the complex mode of wave propagation it gives rise to a relatively simple spatial pattern of average cAMP, which can be read out by the cells in different positions in the slug to keep the differentiation state of the cells in the slug stable (Fig. 7D).

These simulations suggest that the wave propagation pattern is not only responsible for the control of cell movement but also might be involved in the differentiation of the prestalk cell types [58].

## 6. Tip formation, cell differentiation and sorting

One of the most interesting but also most complicated phases of development is slug formation. During aggregation the cell density increases dramatically and cells start to move up on top of each other in the third dimension. In the mound cells begin to differentiate in prestalk and prespore cells at random positions. The prestalk cells then sort towards the top of the mound to form a tip [63]. The mound then contracts at the base while extending up in the air to form a standing slug. Slug formation can be seen as a two-step process, i.e. sorting of prestalk cells to form a tip followed by a tip induced contraction and elongation of the mound to form a standing slug (Fig. 1).

Cell sorting most likely results from differential chemotactic cell movement towards cAMP. Experiments showed that prestalk cells preferentially sort towards an artificial cAMP source [64]. Furthermore mutants which overexpress cAMP phosphodiesterase are blocked at the mound stage of development and defective in cell sorting [52]. The difference in effective movement speed towards a cAMP source could be caused by cell type specific differences in the motive force generated by prestalk and prespore cells. Differences in motive force could result from differences in the cytoskeleton or cell-cell adhesion, i.e. prespore cells being more adhesive than prestalk cells. There is experimental evidence for both types of mechanisms: isolated *pstA* cells, which will sort to the top of the aggregate, are able to move faster to an

artificial cAMP source than isolated prespore cells [63]. Furthermore several mutants with defects in components of the cytoskeleton are arrested at the mound stage [65,66]. Using a cold sensitive myosin mutant it has been shown, that there are two stages in development where myosin II is absolutely required for morphogenesis, at the mound stage during tip formation and during culmination [67]. Secondly, in multicellular tissues cell-cell interactions are likely to play an important role in the control of cell movement. It is known that prespore cells are more adhesive than prestalk cells [68]. Prestalk cells may therefore move more efficiently in a multicellular aggregate consisting of prespore and prestalk cells. We therefore suspect that cell sorting involves all these mechanisms, i.e. differential chemotaxis towards cAMP, cell type specific differences in the generation of motive force as well as cell type specific differences in cell-cell interactions and cell-substrate interactions.

Cell sorting will feedback on the signalling patterns in the tipped mound since prestalk and prespore cells differ in their excitability. Many experiments suggest that prestalk cells are more excitable than other cells in the mound. Prestalk cells express higher amounts of the enzymes involved in the synthesis and degradation of cAMP, adenylate cyclase and phosphodiesterase [69–71] and they express a specific subset of low affinity cAR2 receptors, which allows them to relay high amplitude cAMP signals, while the expression of the high affinity cAR3 receptor becomes restricted to prespore cells [54,72].

Taken together cell sorting should affect the signalling system in the following way: the collection of fast oscillating prestalk cells in the tip leads to an increased excitability. This causes a loss of spiral arms and the formation of a simple scroll wave in the tip [44]. The removal of the highly excitable prestalk cells from the body of the mound results in a decrease in local excitability and the conversion of the scroll wave in the tip to a twisted scroll wave in the mound [53,58]. This leads to a twisted rotational cell movement in the mound. As a result the mound contracts and extends up into the air.

We are now testing this possibility by an extension of the model from mound formation by incorporation of different cell types (fluids) with different chemotactic and relay properties. We consider the mound to

be a drop of liquid consisting of two kinds of fluids and use a two-field description of this drop to model cell sorting. The velocity of the liquid,  $V$  defined in Eq. (3), is assumed to have two components corresponding to velocities of prestalk,  $V_1$ , and prespore,  $V_2$ , cells:

$$V = (\rho_1 V_1 + \rho_2 V_2) / (\rho_1 + \rho_2) \quad (5)$$

Since the liquid is incompressible:  $\rho_1 + \rho_2 = 1$  in the mound. The chemotactic force,  $F_{ch}$ , in Eq. (3) is also assumed to consist of two components corresponding to chemotactic forcing of prestalk and prespore cells.

$$F_{ch} = (\rho_1 \varphi_1 (\partial g / \partial t) + \rho_2 \varphi_2 (\partial g / \partial t)) \nabla g \quad (6)$$

The difference in cAMP signalling between prestalk and prespore cells is also taken into account by two different sets of parameters for the FitzHugh–Nagumo model. To find the velocities of prestalk and prespore cells we put Eq. (5) and Eq. (6) for velocity and chemotactic force into Eq. (3), put coefficient  $\rho_1 + \rho_2$  to the last term in Eq. (3) and by separating terms consisting  $\rho_1$  and  $\rho_2$  we get two equations for  $V_1$  and  $V_2$ :

$$\partial V_i / \partial t = V_i \nabla (V_i \rho_i) / \rho_i - (V_i \nabla) V + F_i + \eta \Delta (V_i \rho_i) / \rho_i - \nabla p \quad (7)$$

where  $i = 1, 2$

The two equations each coupled with the equation

of conservation of mass (used to define the densities of both fluids) give the evolution of the cell density fields over time. Our preliminary computations show that starting from a random distribution of cell types in the mound one can obtain spatially separated patterns of cell types as well as tip formation. In response to scroll waves rotating along the vertical axis of hemispherical mound the liquid begins to rotate in the opposite direction. The faster moving fluid (prestalk cells) accumulates in the centre and top of the mound. Since the faster fluid is more excitable their separation leads to the mound becoming inhomogeneous with respect to its excitability. This in turn results in a change of the cAMP wave shape. Since the density of the excitable cells is higher on the top of the mound the velocity of wave propagation is higher than in the base of the mound and the scroll becomes twisted. As a consequence the cells experience a vertical chemotactic force which results in the further collection of faster moving cells on the top. Finally all the faster cells collect at the top of the mound and form a tip, exactly as it happens in real mounds (Fig. 8). It seems likely that the model will be able to describe slug migration as resulting from scroll wave propagation and chemotactic cell movement. This is now under investigation. To investigate culmination it will be necessary to include further signalling centres as well as final stalk differentiation.

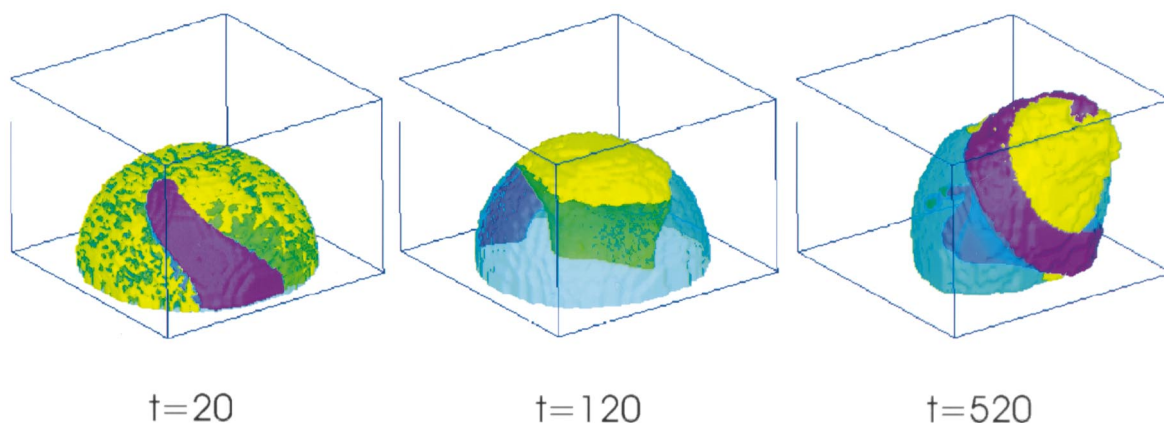


Fig. 8. Simulation of cell sorting and tip formation. To describe cell movement we used Eq. (3), (4), (5), (6) and (7) and to describe cAMP signalling we used the FitzHugh–Nagumo Eq. (1). A sequence of images is shown depicting sorting of highly excitable fast moving prestalk cells (yellow) from less excitable slow moving prespore cells (light green (transparent)) as well as the cAMP signal (pink). A scroll wave was initiated in the mound with an initially random distribution of prestalk and prespore cells. In the course of time the cells sort which results in a twisting of the scroll wave. The period of the scroll wave decreases from 3.8 to 2.1 time units.

## 7. Conclusions

It is now becoming clear that periodic signals not only control aggregation but also all later stages of morphogenesis. Multicellular mounds are organised by either concentric ring waves emanating from one or more centres or by spiral waves with up to ten arms. These signals are most likely used to regulate the process of cell sorting, in which the most excitable cells move on top of the aggregate. This sorting process leads to a highly excitable tip and a less excitable main body. This spatial separation feeds back on the signal geometry. We propose that the cells in the tip are organised by a rotating scroll wave of cAMP with the core of the scroll wave coinciding with the long axis of the tip. The scroll wave converts into a twisted scroll wave and planar waves in the body of the mound. This pattern of wave propagation leads to a rotational movement of the prestalk cells in the tip and a periodic upward movement of the cells in the base of the mound. Furthermore it results in a contraction of the tip and an elongation of the mound into a standing slug which becomes unstable and topples over. The slug now moves away, while the movement of the cells is still being controlled by a scroll wave in the tip and twisted scroll or planar waves in the prespore zone. This pattern of cAMP wave propagation is also used to stabilise prestalk cell type specific gene expression and to initiate stalk differentiation.

*Dictyostelium* is possibly the first organism whose morphogenesis is beginning to be understood at the cellular level. During early development morphogenesis is based on wave propagation in a 2D excitable medium which becomes 3D by chemotactic aggregation of the cells. More complexity is brought into the system as the cells differentiate into several types with different excitable and chemotactic properties. Due to these additional levels of regulation and feedback complicated wave forms such as multi-armed spirals, twisted scroll waves etc. arise.

## Acknowledgements

We like to thank Till Bretschneider for performing the calculations on the wave propagation in slugs. We like to thank Florian Siegert and Jens Rietdorf for

discussion and the BBSRC and Deutsche Forschungsgemeinschaft for financial support.

## References

- [1] G. Weeks, C.J. Weijer, *FEMS Microbiol. Lett.* 124 (1994) 123.
- [2] W.F. Loomis, R. Cann, in: W.F. Loomis (Ed.), *The Development of Dictyostelium discoideum*, Academic Press, New York, 1982, p. 451.
- [3] J. Williams, *Curr. Opin. Genet. Dev.* 5 (1995) 426.
- [4] D. Traynor, M. Tasaka, I. Takeuchi, J. Williams, *Development* 120 (1994) 591.
- [5] C.A. Parent, P.N. Devreotes, *Annu. Rev. Biochem.* 65 (1996) 411.
- [6] M.Y. Chen, R.H. Insall, P.N. Devreotes, *Trends Genet.* 12 (1996) 52.
- [7] R. Kessin, *Microbiol. Rev.* 52 (1988) 29.
- [8] G. Gerisch, *Annu. Rev. Biochem.* 56 (1987) 853.
- [9] R.A. Firtel, *Curr. Opin. Genet. Dev.* 6 (1996) 545.
- [10] F. Alcantara, M. Monk, *J. Gen. Microbiol.* 85 (1974) 321.
- [11] J.D. Gross, M.J. Peacey, D.J. Trevan, *J. Cell Sci.* 22 (1976) 645.
- [12] F. Siegert, C. Weijer, *J. Cell Sci.* 93 (1989) 325.
- [13] K.J. Tomchik, P.N. Devreotes, *Science* 212 (1981) 443.
- [14] J.J. Tyson, J.D. Murray, *Development* 106 (1989) 421.
- [15] P. Foerster, S. Muller, B. Hess, *Development* 109 (1990) 11.
- [16] A. Goldbeter, *Biochemical Oscillations and Cellular Rhythms. The Molecular Bases of Periodic and Chaotic Behaviour*, Cambridge Universities Press, Cambridge, 1996.
- [17] J.-L. Martiel, A. Goldbeter, *Biophys. J.* 52 (1987) 807.
- [18] J.L. Martiel, A. Goldbeter, *Lect. Notes Biomath.* 71 (1987) 244.
- [19] Y.H. Tang, H.G. Othmer, *Math. Biosci.* 120 (1994) 25.
- [20] Y.H. Tang, H.G. Othmer, *Phil. Trans. R. Soc. Lond. B* 349 (1995) 179.
- [21] J.M. Mato, A. Losada, V. Nanjundiah, T.M. Konijn, *Proc. Natl. Acad. Sci. USA* 72 (1975) 4991.
- [22] G. Gerisch, *Biol. Cellulaire* 32 (1978) 61.
- [23] M.J. Caterina, P.N. Devreotes, *FASEB J.* 5 (1991) 3078.
- [24] D. Wessels, D. Shutt, E. Voss, D.R. Soll, *Mol. Biol. Cell* 7 (1996) 1349.
- [25] D. Wessels, J. Murray, D.R. Soll, *Cell Motil. Cytoskel.* 23 (1992) 145.
- [26] E.F. Keller, L.A. Segel, *J. Theor. Biol.* 26 (1970) 399.
- [27] B. Novak, F.F. Seelig, *J. Theor. Biol.* 56 (1976) 301.
- [28] S.A. Mackay, *J. Cell Sci.* 33 (1978) 1.
- [29] O.O. Vasieva, B.N. Vasiev, V.A. Karpov, A.N. Zaikin, *J. Theor. Biol.* 171 (1994) 361.
- [30] C. van Oss, A.V. Panfilov, P. Hogeweg, F. Siegert, C.J. Weijer, *J. Theor. Biol.* 181 (1996) 203.
- [31] H. Levine, W. Reynolds, *Phys. Rev. Lett.* 66 (1991) 2400.
- [32] B.N. Vasiev, P. Hogeweg, A.V. Panfilov, *Phys. Rev. Lett.* 73 (1994) 3173.
- [33] T. Hofer, P.K. Maini, *Phys. Rev. E* 56 (1997) 2074.

- [34] T. Hofer, J.A. Sherratt, P.K. Maini, *Proc. R. Soc. Lond. Ser. B Biol. Sci.* 259 (1995) 249.
- [35] B.M. Shaffer, *Am. Naturalist* 91 (1957) 19.
- [36] V. Nanjundiah, *J. Theor. Biol.* 42 (1973) 63.
- [37] N.J. Savill, P. Hogeweg, *J. Theor. Biol.* 184 (1997) 229.
- [38] F. Siegert, C.J. Weijer, *Curr. Biol.* 5 (1995) 937.
- [39] J. Rietdorf, F. Siegert, C.J. Weijer, *Dev. Biol.* 177 (1996) 427.
- [40] M. Jacquet, R. Guilbaud, H. Garreau, *Mol. Gen. Genet.* 211 (1988) 441.
- [41] M.J. Caterina, J.L.S. Milne, P.N. Devreotes, *J. Biol. Chem.* 269 (1994) 1523.
- [42] G. Gerisch, *Naturwiss* 58 (1971) 430.
- [43] J. Rietdorf, F. Siegert, S. Dharmawardhane, R.A. Firtel, C.J. Weijer, *Dev. Biol.* 181 (1997) 79.
- [44] B.N. Vasiev, F. Siegert, C.J. Weijer *Phys. Rev. Lett.* 78 (1997) 2489.
- [45] B. Vasiev, F. Siegert, C.J. Weijer, *J. Theor. Biol.* 184 (1997) 441.
- [46] A.J. Durston, F. Vork, C. Weinberger, in: J.G. Vassileva-Popova, E.V. Jensen (Eds.), *Biophysical and Biochemical Information Transfer in Recognition*, Plenum Press, New York, 1979, p. 693.
- [47] F. Siegert, C.J. Weijer, *Physica D* 49 (1991) 224.
- [48] F. Siegert, C.J. Weijer, *Proc. Natl. Acad. Sci. USA* 89 (1992) 6433.
- [49] D. Dormann, C. Weijer, F. Siegert, *J. Cell Sci.* 110 (1997) 1831.
- [50] P. Schaap, M. Wang, *Dev. Biol.* 105 (1984) 470.
- [51] B. Wang, A. Kuspa, *Science* 277 (1997) 251.
- [52] D. Traynor, R.H. Kessin, J.G. Williams, *Proc. Natl. Acad. Sci. USA* 89 (1992) 8303.
- [53] O. Steinbock, F. Siegert, S.C. Muller, C.J. Weijer, *Proc. Natl. Acad. Sci. USA* 90 (1993) 7332.
- [54] Y.M. Yu, C.L. Saxe, *Dev. Biol.* 173 (1996) 353.
- [55] G.T. Ginsburg, A.R. Kimmel, *Genes Dev.* 11 (1997) 2112.
- [56] L. Wu, J. Franke, R.L. Blanton, G.J. Podgorski, R.H. Kessin, *Dev. Biol.* 167 (1995) 1.
- [57] A.L. Hall, J. Franke, M. Faure, R.H. Kessin, *Dev. Biol.* 157 (1993) 73.
- [58] T. Bretschneider, F. Siegert, C.J. Weijer, *Proc. Natl. Acad. Sci. USA* 92 (1995) 4387.
- [59] K.A. Jermyn, K.T. Duffy, J.G. Williams, *Nature* 340 (1989) 144.
- [60] M. Berks, R.R. Kay, *Development* 110 (1990) 977.
- [61] N.A. Hopper, C. Anjard, C.D. Reymond, J.G. Williams, *Development* 119 (1993) 147.
- [62] R.D.M. Soede, N.A. Hopper, J.G. Williams, P. Schaap, *Dev. Biol.* 177 (1996) 152.
- [63] A. Early, T. Abe, J. Williams, *Cell* 83 (1995) 91.
- [64] S. Matsukuma, A.J. Durston, *J. Embryol. Exp. Morphol.* 50 (1979) 243.
- [65] A. De Lozanne, J.A. Spudich, *Science* 236 (1987) 1086.
- [66] F. Rivero, B. Koppel, B. Peracino, S. Bozzaro, F. Siegert, C.J. Weijer, M. Schleicher, R. Albrecht, A.A. Noegel, *J. Cell Sci.* 109 (1996) 2679.
- [67] M.L. Springer, B. Patterson, J.A. Spudich, *Development* 120 (1994) 2651.
- [68] C.H. Siu, R.K. Kamboj, *Dev. Genet.* 11 (1990) 377.
- [69] S.S. Brown, C.L. Rutherford, *Differentiation* 16 (1980) 173.
- [70] M. Pahlic, C.L. Rutherford, *J. Biol. Chem.* 254 (1979) 9703.
- [71] C. Rutherford, S. Brown, D. Armant, *Adv. Cycl. Nucl. Res.* 14 (1981) 705.
- [72] C.L. Saxe III, Y.M. Yu, C. Jones, A. Bauman, C. Haynes, *Dev. Biol.* 174 (1996) 202.
- [73] B. Vasiev, F. Siegert, C. Weijer, *Phys. Rev. Lett.* 78 (1997) 2489.